


CONF-780829--10

CLASSIFICATION		DOCUMENT IDENTIFICATION NO. PNL-SA-6831 PT2	
 Battelle Pacific Northwest Laboratories Richland, Washington 99352		COPY AND SERIES NO.	
		DATE AUGUST 1978	
TITLE AND AUTHOR SPECULARITY MEASUREMENTS FOR SOLAR MATERIALS M. A. LIND, J. S. HARTMAN AND H. L. HAMPTON		CONTRACT <input type="checkbox"/> - 1830 <input type="checkbox"/> - 1831	
		PROJECT NO. RESERVED FOR TECH. INFO. USE	

MASTER

D I S T R I B U T I O N					
NAME	COMPANY	LOCATION	NAME	COMPANY	LOCATION
			<p>NOTICE MN ONLY</p> <p>PORTIONS OF THIS REPORT ARE ILLEGIBLE. It has been reproduced from the best available copy to permit the broadest possible avail- ability.</p>		
			<p>NOTICE</p> <p>This report was prepared as an account of work sponsored by the United States Government. Neither the United States nor the United States Department of Energy, nor any of their employees, nor any of their contractors, subcontractors, or their employees, makes any warranty, express or implied, or assumes any legal liability or responsibility for the accuracy, completeness or usefulness of any information, apparatus, product or process disclosed, or represents that its use would not infringe privately owned rights.</p>		
			<p>DISTRIBUTION OF THIS DOCUMENT IS UNLIMITED</p>		

ROUTE TO	PAYROLL NO.	COMPANY	LOCATION	FILES ROUTE DATE	SIGNATURE AND DATE

DISCLAIMER

This report was prepared as an account of work sponsored by an agency of the United States Government. Neither the United States Government nor any agency Thereof, nor any of their employees, makes any warranty, express or implied, or assumes any legal liability or responsibility for the accuracy, completeness, or usefulness of any information, apparatus, product, or process disclosed, or represents that its use would not infringe privately owned rights. Reference herein to any specific commercial product, process, or service by trade name, trademark, manufacturer, or otherwise does not necessarily constitute or imply its endorsement, recommendation, or favoring by the United States Government or any agency thereof. The views and opinions of authors expressed herein do not necessarily state or reflect those of the United States Government or any agency thereof.

DISCLAIMER

Portions of this document may be illegible in electronic image products. Images are produced from the best available original document.

SPECULARITY MEASUREMENTS FOR SOLAR MATERIALS*

M. A. Lird, J. S. Hartman and H. L. Hampton
Pacific Northwest Laboratory
Richland, Washington 99352

Abstract

A technique using Fourier transform analysis which is suitable for measuring the specularity of solar glass components in the mrad and sub-mrad is discussed and demonstrated. A brief mathematical background as well as illustrative examples are included. A number of methods for image analysis are discussed with particular emphasis given to electronic integrating detectors. Typical Fourier plane image distributions are given for a few common solar utilization materials and details of the instrument used to produce the images are considered. The limitations and capabilities of various instruments are outlined along with methods for further enhancing the utility and sensitivity of the technique.

Introduction

In many solar applications, particularly those using concentrating collectors, the specularity of the transmissive or reflective collector material can be a significant parameter limiting the overall performance and efficiency of the system. The specific requirements for the specularity of the collector materials are system dependent and are usually determined by the angular aperture of the receiver as viewed from the collector.

In heliostat applications the effective angular aperture of the receiver could be as small as 9.5 mrad, the angular divergence of the sun. Only highly specular materials should be used in these applications. In other systems, such as the augmented flat plate collectors which incorporate relatively large receivers and short reflector to receiver distances, less specular materials may be adequate.

This paper describes how the Fourier transforming properties of a simple lens can be used to examine the scattering function or specularity of these solar collector materials. It also discusses the practical implementation of the Fourier transform approach to real measurement instrumentation, its ramifications and limitations.

Mathematical Background

The basic principles for characterizing the specularity of solar materials using Fourier Transform techniques have been employed by several investigators⁽¹⁻⁴⁾ for a number of years. A typical instrument is illustrated schematically in Figure 1. It consists of a light source, collimation optics, collection optics, and some kind of detector located at or near the image plane.

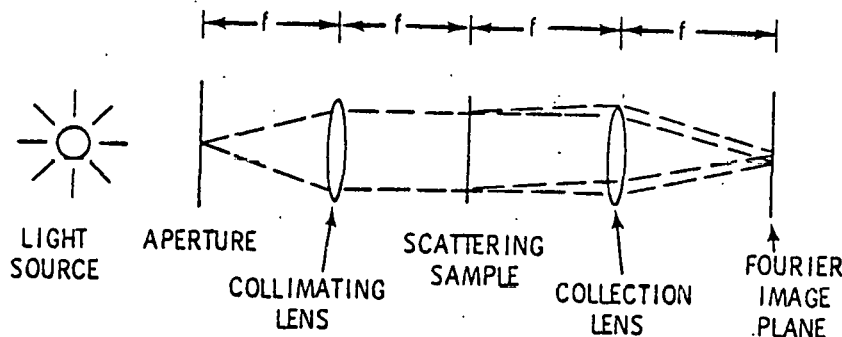


Fig. 1. Typical optical Fourier transform examination instrument.

This type of optical arrangement can be described mathematically using a generalized system approach. The interactions due to each of the elements in Figure 1 can be represented in block form as shown in Figure 2. In this figure $\psi(x,y; s_1)$ is the input wave function, $f(x,y)$ is an aperture function in the P_1 plane, $g(c,d)$ is the transmission or reflection function of the scattering material under investigation, P_2 and P_4 are the lens planes, and $h(m,n)$ is the resulting field function in the P_5 plane.

By representing the action of the lenses and the physical propagation of the light as elements in a generalized system, the mathematical analysis of this system can be simplified. In the notation of A. Vander Lugt⁽⁵⁾, a lens is equivalent to the physical space multiplier as shown in Equation 1 and is denoted by the multiplication symbol \otimes .

* Prepared for the U.S. Department of Energy under Contract EX-76-C-06-1830.

SPECULARITY MEASUREMENTS FOR SOLAR MATERIALS*

M. A. Lird, J. S. Hartman and H. L. Hampton
Pacific Northwest Laboratory
Richland, Washington 99352

Abstract

A technique using Fourier transform analysis which is suitable for measuring the specularity of solar glass components in the mrad and sub-mrad is discussed and demonstrated. A brief mathematical background as well as illustrative examples are included. A number of methods for image analysis are discussed with particular emphasis given to electronic integrating detectors. Typical Fourier plane image distributions are given for a few common solar utilization materials and details of the instrument used to produce the images are considered. The limitations and capabilities of various instruments are outlined along with methods for further enhancing the utility and sensitivity of the technique.

Introduction

In many solar applications, particularly those using concentrating collectors, the specularity of the transmissive or reflective collector material can be a significant parameter limiting the overall performance and efficiency of the system. The specific requirements for the specularity of the collector materials are system dependent and are usually determined by the angular aperture of the receiver as viewed from the collector.

In heliostat applications the effective angular aperture of the receiver could be as small as 9.5 mrad, the angular divergence of the sun. Only highly specular materials should be used in these applications. In other systems, such as the augmented flat plate collectors which incorporate relatively large receivers and short reflector to receiver distances, less specular materials may be adequate.

This paper describes how the Fourier transforming properties of a simple lens can be used to examine the scattering function or specularity of these solar collector materials. It also discusses the practical implementation of the Fourier transform approach to real measurement instrumentation, its ramifications and limitations.

Mathematical Background

The basic principles for characterizing the specularity of solar materials using Fourier Transform techniques have been employed by several investigators⁽¹⁻⁴⁾ for a number of years. A typical instrument is illustrated schematically in Figure 1. It consists of a light source, collimation optics, collection optics, and some kind of detector located at or near the image plane.

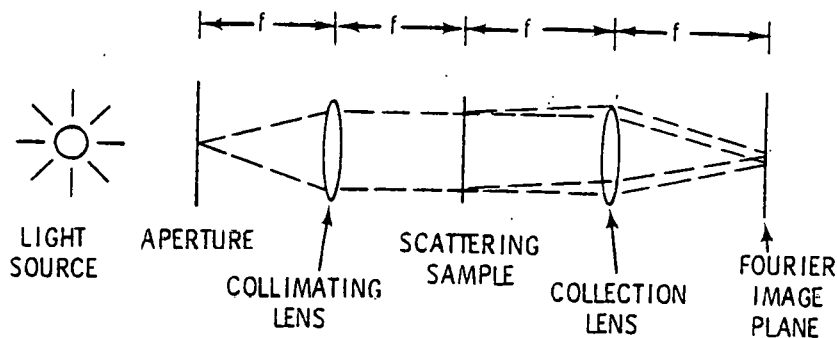


Fig. 1. Typical optical Fourier transform examination instrument.

This type of optical arrangement can be described mathematically using a generalized system approach. The interactions due to each of the elements in Figure 1 can be represented in block form as shown in Figure 2. In this figure $\psi(x,y; s_1)$ is the input wave function, $f(x,y)$ is an aperture function in the P_1 plane, $g(c,d)$ is the transmission or reflection function of the scattering material under investigation, P_2 and P_4 are the lens planes, and $h(m,n)$ is the resulting field function in the P_5 plane.

By representing the action of the lenses and the physical propagation of the light as elements in a generalized system, the mathematical analysis of this system can be simplified. In the notation of A. Vander Lugt⁽⁵⁾, a lens is equivalent to the physical space multiplier as shown in Equation 1 and is denoted by the multiplication symbol \otimes .

* Prepared for the U.S. Department of Energy under Contract EY-76-C-06-1830.

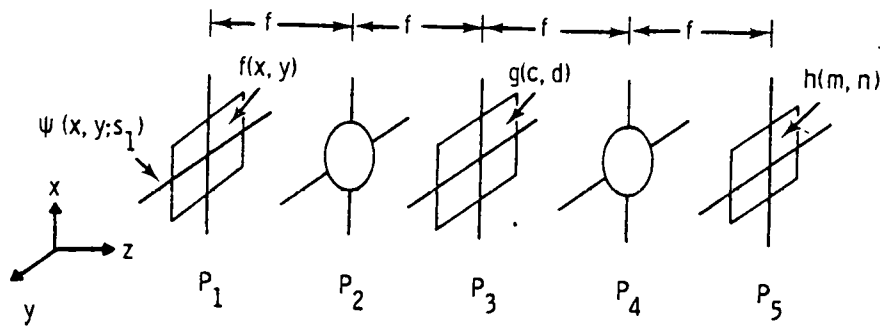


Fig. 2. Interaction representation of instrument shown in Figure 1.

$$L(x, y) = \exp \left[-j \frac{k}{2f} (x^2 + y^2) \right] \quad (1)$$

Here k is the wave number of the light, f is the focal length of the lens and the x and y coordinates are orthogonal to z , the optical axis of the system. Propagation is equivalent to a physical space convolution which is represented in this notation as a box, $\boxed{}$.

The notation is applied by defining a canonical function and its conjugate. Let

$$\psi(x, y; s) \equiv \exp \left[j \frac{ks}{2} (x^2 + y^2) \right] = \bar{\psi}(x, y; -s) \quad (2)$$

where s is a reciprocal distance given as either

$$s = \frac{1}{f} = \hat{f} \quad (3)$$

when describing the interaction with a lens of focal length f , or

$$s = \frac{1}{z} \quad (4)$$

when describing spatial propagation.

Using this notation, a mathematical representation of each of the elements in the system depicted in Figure 2 can be written as shown in Figure 3. Here we have assumed that each element in the optical system is separated by a distance f , corresponding to the focal lengths of the two identical lenses. The multiplication symbols represent the product of two elements using a common set of variables. The convolution rectangles represent the integral of the product of an input function and a modified ψ function. This convolution term is written as the input variables minus the output variables integrated over the input variables.

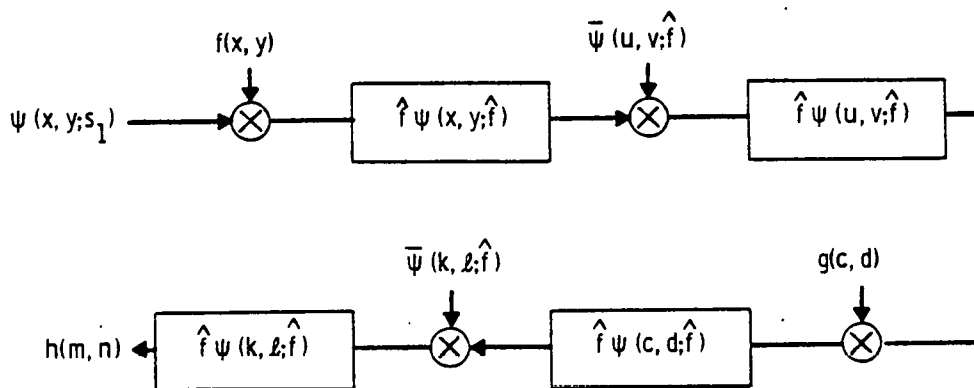


Fig. 3. Generalized system representation of instrument shown in Figure 2.

More explicitly, the equation for our simple optical system becomes:

$$\begin{aligned}
 h(m,n) = & \hat{f}^4 \iiint_{P_1} \iiint_{P_2} \iiint_{P_3} \iiint_{P_4} \psi(x,y;s_1) f(x,y) \psi(x-u,y-v;\hat{f}) \\
 & \times \bar{\psi}(u,v;\hat{f}) \psi(u-c,v-d;\hat{f}) g(c,d) \psi(c-k,d-l;\hat{f}) \\
 & \times \bar{\psi}(k,l;\hat{f}) \psi(k-m,l-n;\hat{f}) \delta x \delta y \delta u \delta v \delta c \delta d \delta k \delta l
 \end{aligned} \quad (5)$$

this equation can be simplified by substituting the functional forms of ψ and $\bar{\psi}$ into the equation, utilizing the basic symmetry and algebraic properties of these canonical functions⁽⁶⁾, and integrating. The resulting expression is:

$$\begin{aligned}
 h(m,n) = & -\lambda^2 \hat{f}^2 \iint_{P_1} \iint_{P_3} \psi(x,y;s_1) f(x,y) \exp \left[-jk\hat{f}(xc + yd) \right] \\
 & \times g(c,d) \exp \left[-jk\hat{f}(cm + dn) \right] \delta x \delta y \delta c \delta d
 \end{aligned} \quad (6)$$

In the special case where the aperture function, $f(x,y)$, has a small enough spatial extent to be approximated by a delta function and the input wave function, $\psi(x,y;s_1)$ is a plane wave. The equation simplifies further to:

$$h(m,n) = \kappa \iint_{P_3} g(c,d) \exp \left[-jk\hat{f}(cm + dn) \right] \delta c \delta d \quad (7)$$

Here κ is a function of the wavelength of the incoming radiation and the focal length of the lenses.

Equation (7) shows that under the conditions of monochromatic planewave illumination and very small entrance aperture dimensions (collimated sample illumination) the intensity distribution at the image plane P_5 is the exact Fourier transform of the transmission or reflection function, $g(c,d)$, of the material placed at the sample plane, P_3 .

In practice it may not be desirable to implement sufficiently small apertures in the plane P_1 to use a delta function approximation. In this case it is necessary to revert back to equation (6). The finite size of the aperture results in an intensity distribution at P_5 that is a convolution of the normalized aperture transmission profile, $f(x,y)$, with the Fourier transform of the transmission or reflection function of the sample.

The deconvolution of this image intensity distribution to determine the actual scattering function of the sample may be mathematically complex. However, with a few reasonable assumptions about the functional form of $g(c,d)$, the problem becomes manageable and the results useful. For example, the work performed by Pettit⁽²⁾ assumes a Gaussian distribution for the scattering function of the material. Different materials can then be compared with each other on the basis of a two parameter (peak height and full width at half maximum) best-fit approximation to the Gaussian scattering distribution. In practice, multiple distributions may actually be necessary to best characterize the material, but the technique works well with a wide variety of materials.

Fourier Image

In order to illustrate the basic image properties and the utility of the Fourier transform technique for comparing materials, let us first examine some well known idealized geometrical configurations and their corresponding Fourier images. On the left hand side of Figure 4 are the transmission shadowgraphs of three simple patterns, a one-dimensional periodic transmission grating, a two-dimensional periodic screen grating, and a two-dimensional periodic screen with some random noise spots superimposed. On the right side of the figure are the corresponding Fourier images. Notice particularly the symmetry properties of the transforms compared to the original objects.

One-dimensional structures in the sample plane result in the Fourier transform features along an axis orthogonal to the structure. Periodicity in the sample structure produces features at discrete locations in the transform plane. Similar features can be noted for the two-dimensional case. Random noise introduced into the regular structure causes blurring of the discrete features in the Fourier plane.

Figure 5 illustrates two samples which are more nearly representative of the actual processing defects found in many extruded or polished solar materials. The shadowgraphs shown are transparent plastic materials which have been scratched preferentially along one (Fig. 5a) or two (Fig. 5c) axes. The resulting Fourier images again retain the basic symmetry of the shadowgraph images but the individual spots are blurred due to the non-periodic nature of the scratches.

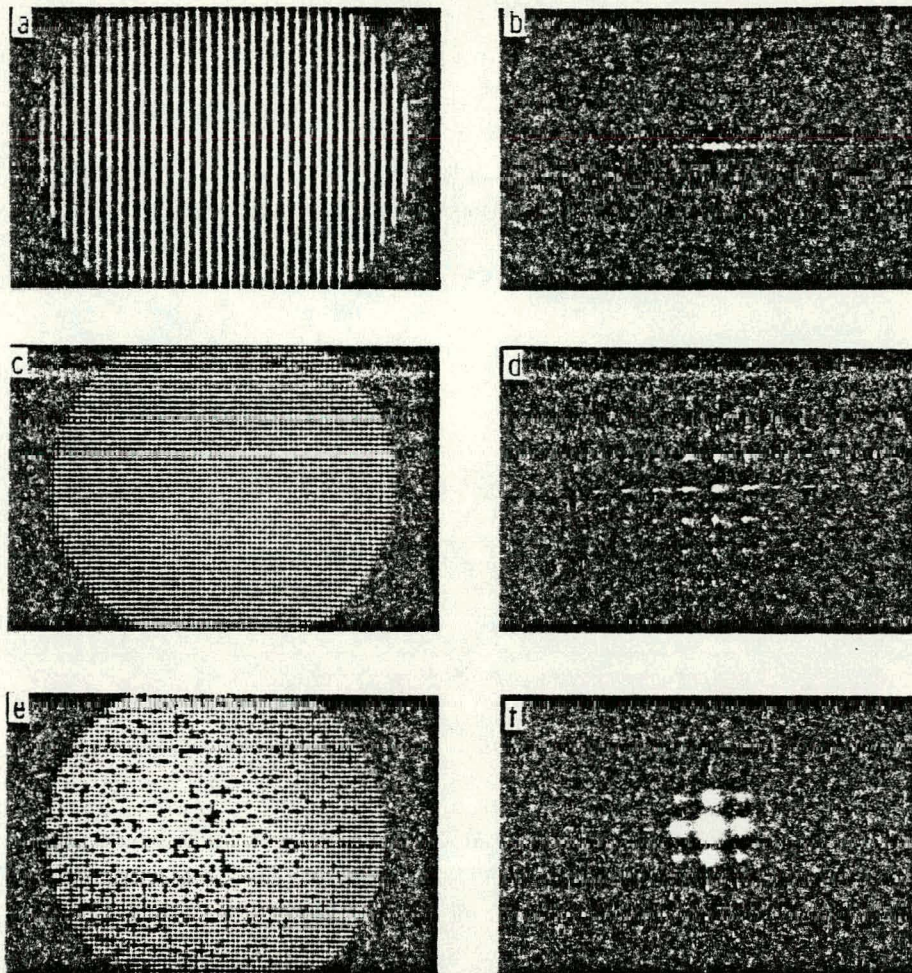


Fig. 4. Transmission shadowgraphs of three gratings and their corresponding Fourier plane images: a&b) one-dimensional periodic transmission grating, c&d) two-dimensional periodic transmission grating, e&f) two-dimensional grating with random noise superimposed.

To further illustrate the utility of this technique, Figure 6 shows the Fourier transform images of three actual materials that have been investigated; a) float glass, b) an extruded polytetrafluorethylene sheet, and c) a polycarbonate sheet. The glass is a very specular material as evidenced by the small amount of scatter. The polycarbonate exhibits asymmetry in several directions and is, in general, not as specular as the glass. The polytetrafluorethylene exhibits strong preferential processing marks.

A more quantitative and perhaps more useful analysis can be performed by examining the image in detail. In general, the light incident on the Fourier plane is displaced from the optical axis by a distance which is proportional to the tangent of the angle through which it is scattered times the focal length of the lens.

Simple geometrical considerations show that:

$$r = f \tan \phi_{sc} \quad (8)$$

where ϕ_{sc} is the angle through which the light is scattered at the material and r is the radial displacement from the sc optical axis in the Fourier plane.

Thus it is possible to map the angular scattering distribution of the material given the measurement system geometry and the intensity distribution in the Fourier plane. In terms of the Fourier images shown in Figure 6, one can readily compare the relative scattering properties of the materials since the photographs were taken under the same geometrical and illumination conditions.

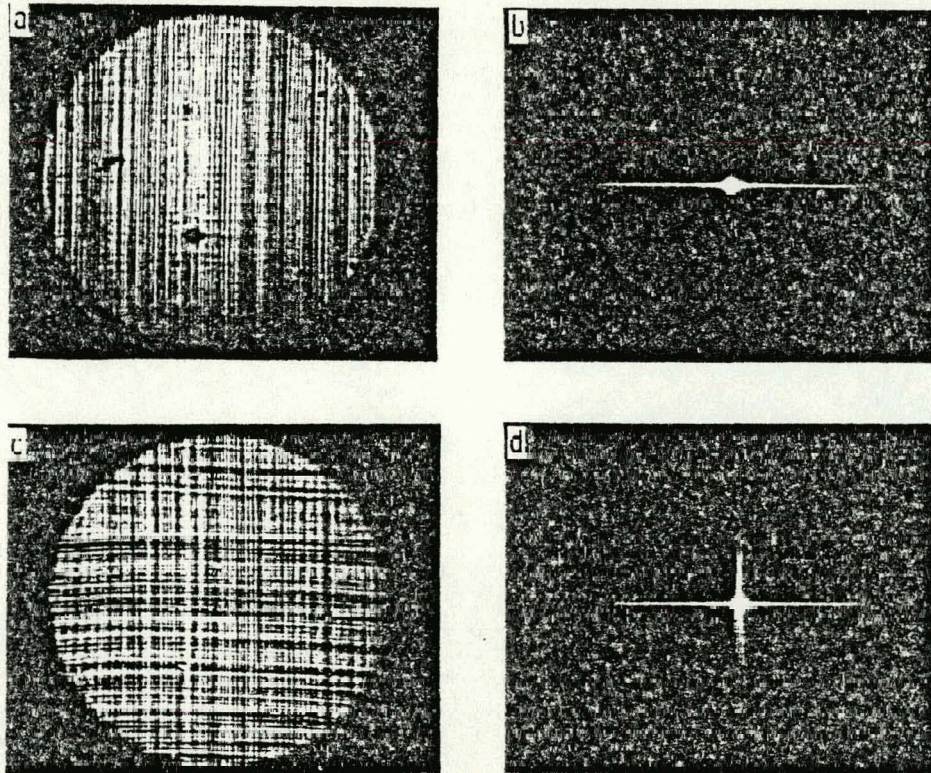


Fig. 5. Shadowgraphs and Fourier images of scratched transparent materials: a&b) one dimensional, c&d) two dimensional, skewed in one dimension.

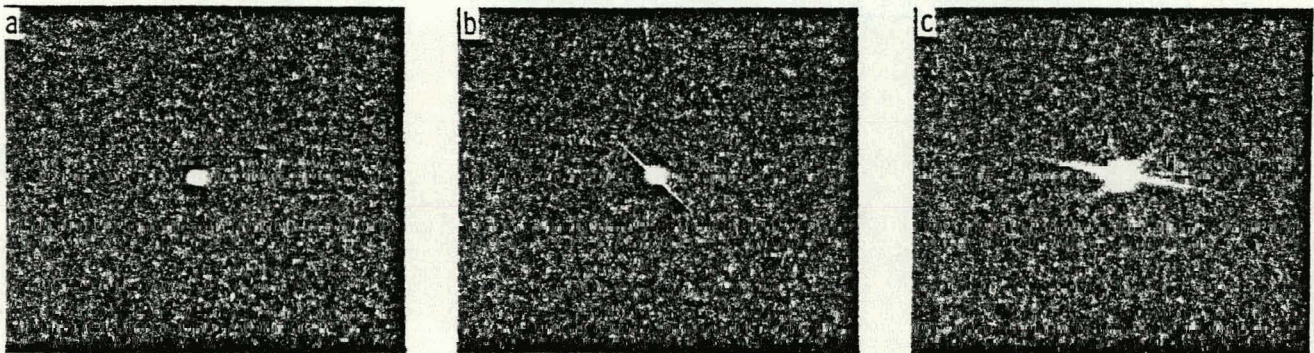


Fig. 6. Fourier plane images of a) float glass, b) polytetrafluorethylene sheet, and c) polycarbonate sheet.

Image Analysis

More detailed information about the distribution of the scattered light and consequently the scattering function of the material can be obtained by analysing the Fourier image in greater detail. A variety of techniques can be employed, each with its own advantages and disadvantages. These techniques can be divided into three categories: 1) one-dimensional sampling, 2) two-dimensional sampling and 3) integrated sampling.

When sampling in one dimension, the intensity distribution along a single line in the Fourier plane is measured. Detection systems that have been used include small aperture scanning detectors and linear diode arrays⁽¹⁾. The resolution of such systems is limited by the finite size of the aperture or the dimensions of the individual sensitive elements of the array. This technique provides useful intensity profile information for materials with isotropic scattering distributions, but it may yield misleading results in those materials which scatter anisotropically. System alignment is critical since small displacements of the detector off the optical axis may also produce misleading results. However, one-dimensional techniques do lend themselves to relatively simple reduction of data into useful engineering quantities since the data is generally more easily interpreted than in the more complex two-dimensional sampling techniques.

When sampling in two dimensions, it is possible to measure the spatial variations in intensity in the entire Fourier plane simultaneously. Anisotropic materials can be fully characterized at the expense of added data processing. Also the alignment of two-dimensional detectors is usually less critical than in the one-dimensional case since any displacement of the detector off the optical axis only shifts the image. Several

types of detectors that have been used include: photographic film, two-dimensional diode arrays, and conventional raster scan vidicons. Photographic film allows high resolution, but requires relatively long processing times and is not adaptable to real time display. The vidicon and diode array with suitable electronic processing offer the prospect of contour mapping the distribution in the Fourier plane in topographic or isometric formats, but they are limited in resolution due to the limited raster spacing or pixel size in the detector.

When highly specular materials such as glass must be characterized on a real-time basis, the above methods become difficult to implement because of the inherent sensitivity, dynamic range and resolution limits of the detectors. Under these conditions integrating sampling techniques which employ relatively large area detectors and special apertures in the Fourier plane become useful. The primary disadvantage of using the more sensitive integrating system is the loss of some or all information regarding the spatial distribution of the scattering function of the material.

Numerous one and two-dimensional integrating techniques have been used⁽¹⁻⁴⁾ which utilize fixed or adjustable apertures. One technique that is particularly sensitive for screening highly specular materials employs a beam block on the optical axis in the Fourier plane and a photomultiplier detector. The purpose of this spatial filter is to increase the effective sensitivity of the detector to the scattered light by reducing the detected magnitude of the specular beam. The use of the beam block establishes the minimum scattering angle that can be detected; the diameter of the phototube and its distance from the Fourier plane or the diameter of the Fourier transform lens establishes the maximum scattering angle that can be detected. With suitable beam blocks, materials that scatter in the mrad and sub-mrad range can be examined. This type of device is especially useful as a screening and comparison tool for high specular materials.

Experimental Considerations

A practical Fourier transform system was assembled as shown in Figure 7 for the examination of high specular materials. In this application most of the incident beam is transmitted without alteration while a small fraction of the energy is scattered. The resulting image in the Fourier plane can then be thought of as a superposition of these two beam components. The transmission of a beam through the solar material is somewhat different than transmission through a standard aperture in that an aperture modulates only the amplitude of the beam. Materials, on the other hand, will generally modulate both the phase and amplitude of the transmitted wave.

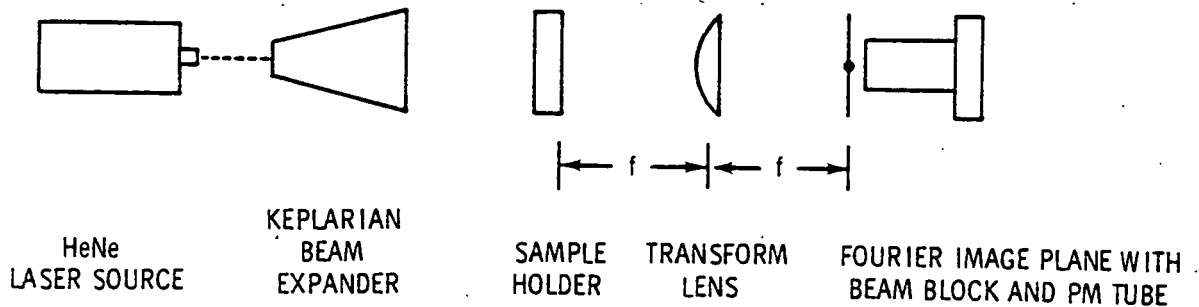


Fig. 7. Illustration of practical optical Fourier transform system.

If the material sample was perfectly planar and homogeneous it would not alter the nature of the beam incident on the Fourier transform lens. The Fourier transform would then be determined by the finite radius of the input beam and would be the well-known Bessel function solution of the diffraction limited spot for a circular beam. But the material alters the beam to some extent and the resulting beam then contains components of both the unaltered and the scattered light. The unaltered specular beam image is not related to the material inhomogeneities. Materials causing scatter increase the intensity of the Fourier image outside the diffraction pattern from the unaltered beam.

In an attempt to separate the scattered image from the specular beam image, it is useful to examine the radial dependence of each image in the Fourier image plane. First, consider the diffraction limited spot resulting from the specularly transmitted beam. The image intensity at a point P in the Fourier plane as found in Born and Wolf⁽⁷⁾ is:

$$I(r) = I_0 \left[\frac{2J_1(kar)}{kar} \right]^2 \quad (9)$$

Here J_1 is the first order Bessel function, a is the radius of circular input beam, k is the wave number and equals $2\pi/\lambda$, and r is the radius from the optical axis to the observation point P.

The fraction of the total beam energy passing within a circle of radius r is given by:

$$L(r) = 1 - J_0^2(kar) - J_1^2(kar) \quad (10)$$

The first minimum occurs at:

$$r_1 = 1.22 \frac{a}{2a} \quad (11)$$

Where f is the focal length of the lens.

The second and third minimas occur at $1.83r_1$ and $2.66r_1$, respectively. The power passing outside r has been calculated for the first 20 minima's of equation (8) and are plotted in Figure 8 as a function of (r/r_1) . An examination of the graph shows that by blocking the central portion of the beam at the focal point the majority of the specular energy can be prevented from reaching the detector. The particular system used in this study employed an expanded collimated 6328Å laser source, and a Fourier transforming lens with a focal length of 200mm and a diameter of 50mm. The incident beam was apertured down to approximately 680 mils. Using equation (10), one finds $r_1 = 0.35$ mils ($8.9 \mu\text{m}$). This value has been used to scale the horizontal axis in Figure 8 into both Fourier plane radius and, with the aid of equation (8), scattering angle ϕ_{sc} . The actual selection of a beam block size will be a compromise between the desire to reduce the specular beam level and to measure the effects of small angle scattering. The effects of a circular beam block with a 5 mil (0.13mm) radius in this system can be determined by examination of Figure 8. For these optics less than 1.2% of the specular beam will reach the detector and light scattered less than 0.65 mrad will also be blocked.

A second consideration for the practical optical system is the bandwidth of the overall system. This is governed by the optical elements and the detector. For a sample with periodic structure, the scattering angle for the beam can be directly related to the sample periodicity using diffraction theory. For a one-dimensional grid, the first order, (smallest angle), diffracted intensity maximum occurs at an angle θ which satisfies:

$$\sin \theta = \pm \lambda / h \quad (12)$$

where h is the grid spacing. This equation can be inverted to determine the grid spacing that corresponds to specific diffraction angles. An experimental system will have a limited range of scattered angles that can be detected and resolved. The maximum angle is frequently determined by the maximum aperture of the lens or the detector. The smallest angle may be determined by the resolution of the detector or the size of a beam block, if one is used. This angular acceptance range can be used to calculate the detectable range of grid spacings in the sample. Inversion of the grid spacing values will yield the bandwidth limits in the familiar spatial frequency units of lines/mm.

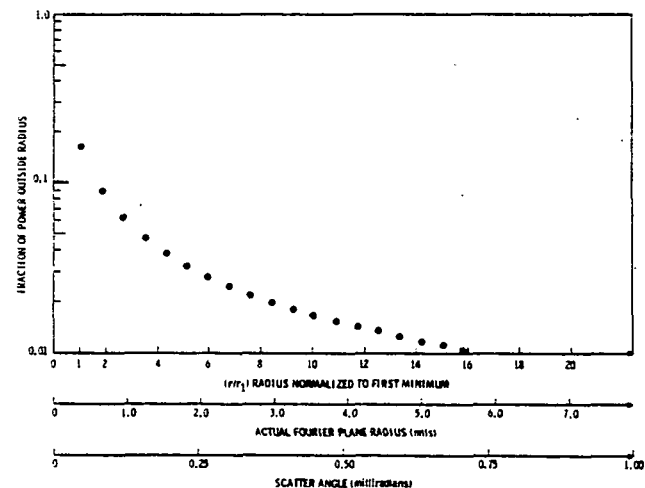


Fig. 8. Fractional power in diffraction limited beam versus a) radius of beam at Fourier plane normalized to first minima, b) actual radius in Fourier plane for 633nm light and 200mm focal length lens, and c) actual scattering angle in milliradians.

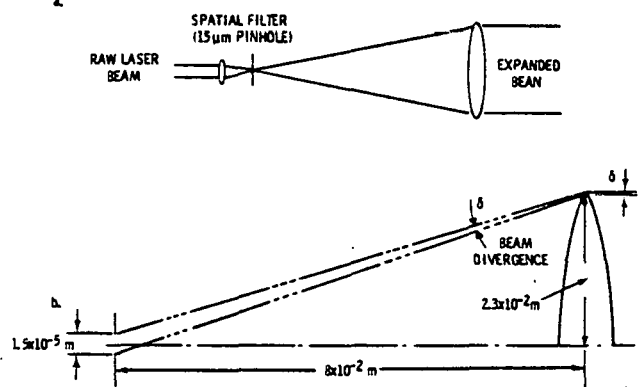


Fig. 9. Geometry of beam expander.

Another potentially limiting factor to the system bandwidth is the diameter of the beam incident on the sample. The beam diameter represents the largest surface period (lowest spatial frequency) that can be determined from the Fourier transform image. The beam diameter must therefore be considered when the low end of the system bandwidth is evaluated.

Since the system has the potential to measure scatter at very small angles, ($1/3$ to $1/2$ milliradian), it is also important to evaluate the divergence of the input beam to determine its significance compared to the small scatter angles under examination. The input laser beam is expanded using a Keplerian beam expander with spatial filtering (Figure 9a). The divergence calculation based on the specific experimental geometry of the beam expander, (Figure 9b), indicates that the divergence varies from 0.17 to 0.19 milliradians depending on the size of the output beam that is used.

A useful beam block is shown in Figure 10. It consists of a 6.2 mil diameter metallic sphere suspended on a 1 mil diameter wire. The sphere is positioned using a precision X-Y-Z translation stage. The sphere blocks roughly 98% of the focused diffraction limited specular light, and all the light scattered by less than $.38 \text{ mrad}$. For the system used in this study the maximum scattering angle detected was 83 milliradians and the photocathode size of the PM tube was the limiting dimension. The lens diameter was large enough so it did not limit the system bandwidth.

A summary of the system limitations for angular acceptance range and spatial frequency bandwidth are shown in Table 1. Values are shown for the PM tube used without a beam block in the Fourier transform plane and with a 6.2 mil beam block. The system dimensions that actually limit the system bandwidth are also identified.

It is important to note that the system is insensitive to misalignment of parallel faced samples when used in the transmission mode. This makes sample alignment non-critical. For materials with parallel faces over the extent of the optical beam, the input and output beams will propagate in the same direction. If the beam is not orthogonal to the sample's surface,

the output beam will be offset slightly from the input beam but they will both focus at the same location in the Fourier plane since they strike the lens at the same angle. Samples with non-parallel faces will give rise to angular beam deflections and subsequent deviation at the Fourier plane.

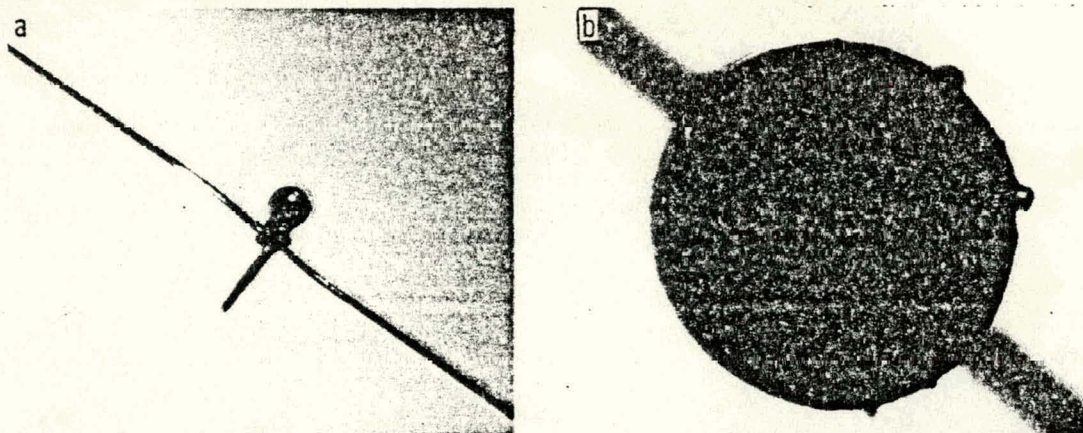


Fig. 10. Photograph of beam block used in experiment showing a) wire support, and b) end view of block.

Table 1. Experimental Optical System Constraints

	FM tube (without beam block)	FM tube (with 6.2 mil beam block)
Angular Acceptance Range (mrad)	0 - 83	0.38 - 83
Spatial Frequency Bandwidth (lines/mm)	0.058 - 131	0.60 - 131
Limiting Factor (Lower band edge)	Beam diameter	Beam block diameter
(Upper band edge)	FM tube aperture	FM tube aperture
Sample Feature Dimensional Range (mils)	0.30 - 680	0.30 - 65.5

Conclusions

An instrument has been assembled and tested to evaluate the scattering properties of optical materials using a spatial filter (circular beam block) in the Fourier transform plane and an integrating detector (FM tube). The instrument has demonstrated sufficiently high sensitivity to be useful in the examination and ranking of glass samples. In fact, the sensitivity of the instrument is sufficient to detect individual scatter center resulting from dust particles on the sample surface. A preliminary survey of glass and plastic materials indicates that better plastics scatter more than 50 times the amount of light scattered by clean glass. One advantage of this type of instrument for evaluating the specularly of transmitting materials is that it is relatively insensitive to sample alignment. The instrument is especially useful in screening or ranking materials based on their intrinsic specularly, but because of the integrating nature of the detector, it does not provide information of the anisotropy of the scattered light. Therefore it can not be used to deduce the scattering functions for different materials.

The instrument design is compact and simple, and should therefore be adaptable to the evaluation of specularly in the field. The basic system design is also capable of increased bandwidth performance by using a larger beam diameter to examine materials with larger structure. A similar system is now being constructed which incorporates a 4 inch diameter beam.

Acknowledgements

The authors would like to acknowledge B. P. Hildebrand and F. R. Reich for their helpful suggestions and contributions.

References

1. H. L. Hampton, J. S. Hartman, M. A. Lind, "Specularity Measurements by Fourier Transform Examination", IES/NBS Solar Seminar on Testing Solar Energy Materials and Systems, Gaithersburg, MD, May 22-24, 1978.
2. R. B. Pettit, "Characterization of the Reflected Beam Profile of Solar Mirror Materials", *Solar Energy* 19, p. 733, 1977.
3. Report D277-10014-1, "Central Receiver Solar Thermal Power System, Collector Sub System Quarterly Technical Progress Report", Boeing Engineering and Construction Company, Seattle, WA, December 31, 1975, p. 81.
4. R. A. Stickley, "Solar Power Array for the Concentration of Energy (SPACE), Semi Annual Progress Report", NSF/RANN/SE/GI-41019/PR/74/12, Sheldahl Inc., Northfield, MN, January 1 - June 30, 1974, pp. 156-159.
5. A. Vander Lugt, "Operational Notation for the Analysis and Synthesis of Optical Data - Processing Systems", *Proc. IEEE* 54, p. 1055, 1966.
6. See for example, F. Paul Carlson, *Introduction to Applied Optics for Engineers*, Academic Press, New York, NY, 1977 p. 58.
7. M. Born and E. Wolf, *Principles of Optics*, the Macmillan Co., New York, NY, 1964.